

# Study of yielding mechanics in nanometer-sized Au contacts

A. Stalder and U. Dürig<sup>a)</sup>

IBM Research Division, Zurich Research Laboratory, CH-8803 Rüschlikon, Switzerland

(Received 7 September 1995; accepted for publication 25 November 1995)

Yielding properties of Au point contacts of nanometer-scale dimensions have been studied using a scanning tunneling microscope supplemented by a force sensor for measuring tip-sample forces. The contacts are made by indenting the tip typically 10 nm into the substrate, whereby an adhesion neck is formed. Three consecutive deformation phases of the neck can be identified during retraction of the tip: (1) buildup of tensile stress, (2) incomplete fracture, and (3) quasicontinuous plastic flow. Finally the neck breaks when a maximum of three to four atoms are left in the contact. In the plastic flow regime, the conductance and thus the contact area shrink exponentially with elongation of the neck, suggesting that plastic deformation occurs locally within 5 to 6 atomic layers. The stress applied during plastic flow is initially of the order of 10 GPa and gradually increases to  $\approx 20$  GPa shortly before the neck breaks. Accounting for a surface force contribution, an intrinsic yield strength of the order of 5 to 8 GPa is obtained, which is more than one order of magnitude larger than the macroscopic yield strength of Au. © 1996 American Institute of Physics. [S0003-6951(96)04705-3]

This letter presents a quantitative study of the yielding mechanics of strained nanometer-sized connective necks formed by indenting a sharp Au tip into a flat Au substrate. Molecular dynamics simulations<sup>1-4</sup> predict that the deformation of such necks proceeds in a series of instabilities that gives rise to characteristic sawtooth-like modulations of the stress-strain characteristics correlating with corresponding changes of the neck diameter. Recently, mechanical instabilities were observed in an experimental study of the plastic deformation of Au contacts having a diameter of typically 3 to 6 nm.<sup>5</sup> These experiments, conducted at 4 K, showed that the contacts deformed in a repetitive sequence consisting of an elastic strain phase followed by a sharply defined yielding event. Depending on the neck diameter, qualitatively different yielding behavior was observed in our experiments, which were performed at room temperature. For necks having a diameter greater than  $\approx 5$  nm, fracture-like yielding prevailed. Here, the neck cross section changes typically by one order of magnitude in catastrophic events. On the other hand, elongation of thin necks having a diameter of less than  $\approx 5$  nm occurred as a quasicontinuous plastic flow. Here, the cross section shrinks exponentially with neck elongation in a repetitive sequence of small steps. This deformation mode can be interpreted in terms of the local order-disorder model proposed by Landman *et al.*<sup>1</sup>

Experiments were conducted under high vacuum conditions ( $p \leq 10^{-6}$  mbar). The applied force and the conductance of the resulting point contact were measured during indentation and retraction of the tip. The apparatus consisted of a scanning tunneling microscope complemented by a stiff force sensor ("nanoguitar"<sup>6</sup>) as sample stage. Thin ( $\approx 200$  nm) (111)-oriented Au films evaporated on glass substrates served as samples, and electrochemically etched Au wires were used as tips. The tips were conditioned *in situ* by ap-

plying a series of short ( $\approx 200$  ms) pulses of a positive bias voltage ( $\approx 100$  V) to the tip during tunneling until a work function of the order of 1 eV was obtained and attractive tip-sample forces not exceeding a few nanonewtons were observed while tunneling.

Tunneling (bias voltage = 10 mV, current = 0.1 nA) is used to define the initial tip-sample distance. An indentation experiment consists of an approach-retraction cycle, which starts with the tip being retracted 1 nm from its tunneling position. Then the tip is ramped 10 nm toward the sample and subsequently retracted by twice the approach distance at a rate of  $2 \text{ nm s}^{-1}$ . Data samples of the tip-sample force and the tip-sample current are taken simultaneously every 10 ms. At the end of one such cycle, the initial tunneling mode is reestablished and the tip is laterally displaced by 10 nm before the next measurement is started. Experimentally, the tip excursion,  $\Delta z$ , is the control parameter. To obtain the actual motion of the tip relative to the sample,  $\Delta s$ , one must correct for the response of the force sensor by using the transformation  $\Delta s = \Delta z - C \Delta F_{\text{TS}}$ , where  $C = 160 \text{ Nm}^{-1}$  is the spring constant of the sensor and  $\Delta F_{\text{TS}}$  denotes the corresponding change of the tip-sample force.

The cross section of the adhesion neck is estimated from the measured conductance using the Landauer-Büttiker formula for ballistic quantum transport<sup>7</sup>:

$$G_c = \frac{2e^2}{h} \sum_{i=1}^{N_c} T_i, \quad (1)$$

where  $N_c$  is the number of conduction channels supported by the contact and the  $T_i$  denotes the transmission probability of the  $i$ th channel. The value of  $N_c$  depends on the electronic structure of the material and on the area of the contact,  $A_c$ . For a free-electron gas, one has  $N_c \approx 4A_c/\lambda_F^2$ . Because  $\lambda_F \approx 2a$ , where  $a$  is the mean interatomic distance, the number of channels corresponds approximately to the number of atoms that fit into the contact cross section (for a valence of one). Theoretical investigations<sup>2</sup> and experiments<sup>8</sup> suggest

<sup>a)</sup> Author to whom correspondence should be addressed. Electronic mail: drg@zurich.ibm.com

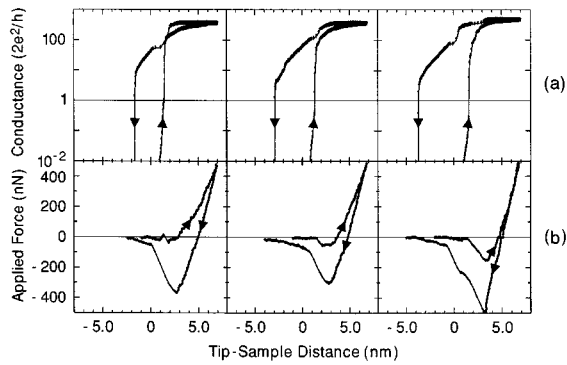


FIG. 1. (a) Conductance on a logarithmic scale and (b) applied force versus tip-sample displacement. Approach and retraction are indicated by arrows.

that elastic interchannel scattering is of minor importance, and one may set  $T_i=1$  in Eq. (1) (which for large  $N_c$  is equivalent to the classical Sharvin conductance<sup>9</sup>). One then obtains  $A_c \approx A_0 g_c$ , where  $A_0 \approx 0.08 \text{ nm}^2$  is the mean area occupied by a Au atom and  $g_c$  is the conductance of the contact in units of  $2e^2/h$  (henceforth, normalization of the conductance will be implicitly assumed).

By their very nature, indentation experiments are not strictly reproducible. However, characteristic features can be identified. Three representative examples of conductance and force data are shown in Fig. 1. During the approach of the tip toward the sample surface, an abrupt transition from tunneling to contact is seen when the tunnel conductance reaches values between 0.2 and 1. Contact manifests itself as a jump of the conductance to values of about 10 to 30, indicating that a connective neck between tip and substrate has been established. The spontaneous neck formation is driven by adhesive surface forces which, in turn, also give rise to the observed overall attractive tip-sample force. As the tip is indented into the substrate, compressive deformation forces build up which eventually dominate, and the overall tip-sample force becomes repulsive.

Irrespective of the details of the indentation process, such as maximum loading force or contact area, three consecutive phases can be distinguished when the tip is retracted after indentation: buildup of tensile stress, incomplete fracture, and plastic flow. Unlike indentation, the neck diameter remains practically constant as the load is relieved during retraction. Thus, there is substantial hysteresis in terms of the shape of the neck. In energetic terms, however, loading and unloading are quasireversible in the compressive stress regime. The mechanical work executed during indentation is to a large degree recovered in the retraction phase, as there is little hysteresis in the corresponding section of the force curves. As the tip is retracted further, tensile stress is built up, yet no significant change of the contact diameter is observed until the tensile stress exceeds a critical value of the order of 10 GPa. Thus, once a neck has been formed it acts like a cylindrical wire whose diameter remains approximately constant up to the point where yielding occurs. The yield point can be identified as the maximum of the tensile force the neck is able to support.

Yielding sets in smoothly as can be seen from the

gradual decrease of the conductance. The shrinking rate of the neck accelerates rapidly, however, as the neck is strained. Simultaneously, the tensile force acting on the tip decreases at a somewhat lower rate than that at which the neck contracts. As a consequence tensile stress escalates up to the point at which this stress can no longer be sustained, and the neck abruptly contracts in a catastrophic event. In some cases a cascade of such events can be observed. The process can be considered as a partial fracture whereby large amounts of elastic strain energy are released in single events. Fracture yielding stops when the neck diameter falls below a critical value of the order of 5 nm (corresponding to a conductance of 200).

Adhesion necks of subcritical dimensions deform in a quasicontinuous manner whereby (1) the conductance decreases exponentially as the neck is elongating, and (2) irrespective of the initial neck size the adhesion neck breaks at a conductance value of typically either  $3 \pm 0.2$  or  $4 \pm 0.2$ . Thus, the cross section of the smallest contacts that can be sustained comprises either three or four atoms. Furthermore, as the initial conditions have no effect on the final deformation process, one suspects that this process involves some kind of a local plastic flow within a limited range of the constriction.

In fact, molecular dynamics simulations performed by Landman *et al.*<sup>1</sup> suggest that plastic yielding of nanometer-sized contacts involves a series of subsequent structural transformations between ordered and disordered states of a small number of atomic layers adjacent to the constriction. In each transformation the neck shrinks as one atomic layer is added. In the spirit of the simulation results we consider yielding steps involving a transformation zone consisting of a fixed number  $n$  of atomic layers, which for simplicity is modeled as a cylindrical section.<sup>10</sup> Only atoms within this zone are able to migrate when the neck yields, whereas atoms outside this zone are assumed to be static.

We now consider a yielding step in which the neck elongates by a distance  $\Delta s$ , and, correspondingly, the cross section shrinks by  $\Delta A_c$ . Hence, a volume  $\Delta A_c n d_0$  is removed from the transformation zone, where  $d_0$  denotes the spacing between atomic layers. This volume of material is incorporated into the rigid section of the neck adjacent to the transformation zone. Hence, because its width is constant, namely  $n d_0$ , a mass balance equation  $-n d_0 \Delta A_c = A_c \Delta s$  can be written. Integration of this equation yields

$$A_c(s) = A_c(s_0) e^{\frac{1}{n d_0} (s_0 - s)}. \quad (2)$$

The cross section of the neck decreases exponentially as the neck is elongated, precisely as observed in the experiment. Measured decay constants  $\kappa = 1/n d_0$  vary between 0.7 and  $1 \text{ nm}^{-1}$ , from which one concludes that plastic flow is confined within a region comprising five to six atomic layers (assuming 0.2 nm for the layer spacing).

The local order-disorder model of plastic flow stipulates that yielding of the neck proceed in a sequence of discrete steps each time a new atomic layer is added to the neck. Indeed, the contact area decreases stepwise as evidenced by the plateaus found in the conductance data (Fig. 2). Previous

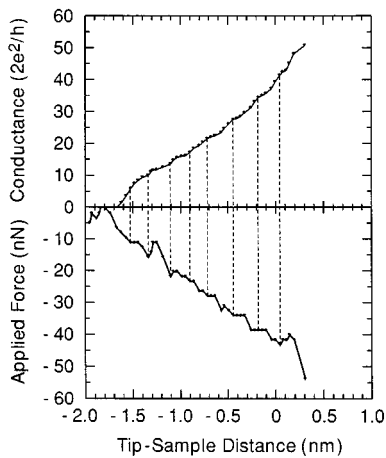


FIG. 2. Conductance and applied force measured in the plastic flow regime shortly before the adhesion neck breaks.

measurements<sup>8</sup> have shown conductance quantization down to single-atom contacts. In our experiments we were not able to sustain contacts containing less than three atoms and, furthermore, quantization effects were as a rule less pronounced than in the published data on Ref. 8. We do not have an explanation for this discrepancy. We would like to point out, however, that conductance plateaus coincide with corresponding fluctuations of the applied force. This provides clear evidence for the notion that the conductance plateaus are connected with discrete structural transformations of the neck, and are not solely a consequence of quantization. As expected for the local order-disorder model, the structure repeats itself quasiperiodically in intervals of  $\Delta s \approx 0.25$  nm, which is close to the lattice spacing of closed-packed planes.

In order to elongate the neck in the plastic flow regime, the apparent contact pressure, defined as the applied force divided by the contact area, must be increased constantly as the neck becomes longer and thinner. Typically, the apparent contact pressure is of the order of 10 GPa for a contact diameter of 2.5 nm ( $g_c \approx 60$ ) and approaches values of the order of 20 GPa shortly before the neck breaks. One is tempted to equate the apparent contact pressure with the yield strength of the neck. However, the applied force contains two contributions, namely a surface force acting at the periphery of the neck plus more or less evenly distributed elastic strain forces. The latter are decisive for yielding to

occur. Therefore, to obtain the intrinsic yield stress  $\sigma_y$ , i.e. the force per unit area which must be applied in order to overcome the internal elastic strain forces at the yield point, the surface force contribution must be subtracted from the applied force. Surface forces are estimated to be of the order of  $2\pi R\Delta\gamma$ , where  $R \approx \sqrt{g_c A_0/\pi}$  is the contact radius and  $\Delta\gamma \approx 3c$  N/m is the free energy associated with a virtual increment of the neck surface. The surface force contribution to the apparent contact pressure is significant. For a contact diameter of 2.5 nm one obtains a value of  $\approx 5$  GPa, which increases to  $\approx 10$  GPa at a diameter of 1 nm. Subtracting this surface force contribution we obtain an intrinsic yield strength of the order of 5 to 8 GPa, which does not depend on the contact diameter. The experimentally determined yield stresses are in very good agreement with corresponding values obtained by Landman *et al.*<sup>1</sup> in their molecular dynamics simulations. It is interesting to note here that the macroscopic yield strength of Au is of the order of 200 MPa. Thus, the rigidity of these nanoscopic necks is more than one order of magnitude larger than that of macroscopic objects.

We would like to thank E. Delamarche for preparing the Au samples. We gratefully acknowledge fruitful discussions with J. Pethica, U. Landman, and J.K. Nørskov. One of us (A.S.) thanks the University of Fribourg (Switzerland) for financial support.

<sup>1</sup>U. Landman, W. D. Luedtke, N. A. Burnham, and R. J. Colton, *Science* **248**, 454 (1990); U. Landman, W. D. Luedtke, *J. Vac. Sci. Technol.* **9**, 414 (1991); U. Landman, W. D. Luedtke, and E. Ringer, *Wear* **153**, 3 (1992).

<sup>2</sup>T. N. Todorov and A. P. Sutton, *Phys. Rev. Lett.* **70**, 2138 (1993).

<sup>3</sup>R. M. Lynden-Bell, *Science* **263**, 1704 (1994).

<sup>4</sup>M. R. Sørensen, K. W. Jacobsen, and P. Stoltze (unpublished).

<sup>5</sup>N. Agrait, G. Rubio, and S. Vieira, *Phys. Rev. Lett.* **74**, 3995 (1995).

<sup>6</sup>A. Stalder and U. Dürig, *Rev. Sci. Instrum.* **66**, 3576 (1995).

<sup>7</sup>M. Büttiker, Y. Imry, R. Landauer, and S. Pinhas, *Phys. Rev. B* **31**, 6207 (1985).

<sup>8</sup>J. M. Krans, J. M. van Ruitenbeek, V. V. Fisun, I. K. Yanson, and L. J. de Jongh, *Nature* **375**, 767 (1995); J. I. Pascual; J. Mendez; J. Gómez-Herrero, A. M. Baró, N. Garcia, U. Landman, W. D. Luedtke, E. N. Bogachek, and H.-P. Cheng, *Science* **267**, 1793 (1995); L. Oleson, E. Laegsgaard, I. Steensgaard, F. Besenbacher, J. Schiøtz, P. Stoltze, K. W. Jacobsen, and J. K. Nørskov, *Phys. Rev. Lett.* **72**, 2251 (1994); N. Agrait, J. G. Rodrigo, and S. Vieira, *Phys. Rev. B* **47**, 12345 (1993).

<sup>9</sup>Y. V. Sharvin, *JETP* **48**, 984 (1965).

<sup>10</sup>Because the constriction corresponds to an extremum of the neck cross section, the derivative of the cross section with respect to the neck axis vanishes at this point. Therefore, the cylinder approximation is correct to the first order.